Tellus (1979), *31*, 447–455

On the dynamics of the equatorial undercurrent

By ROGER L. HUGHES,[1] *Department of Applied Mathematics and Theoretical Physics, University of Cambridge, Cambridge, U.K.*

(Manuscript received April 3; in final form May 29, 1979)

ABSTRACT

Using three different distributions of potential vorticity, it is shown that the velocity field in the equatorial undercurrent is not necessarily unique in an inviscid ocean. The uniqueness of the velocity field is a function of both the thickness of the layer through which the undercurrent flows and the distribution of potential vorticity. For the distributions studied here there is one solution for a large layer thickness. As the layer thickness decreases, a second solution forms. These two solutions then coalesce and vanish as the layer thickness reduces further. Increased baroclinic behaviour qualitatively has the same effect as increased layer thickness. When two solutions are present, the narrower of the solutions widens as the layer thickness decreases, while the wider solution narrows.

1. Introduction

The eastward flowing equatorial undercurrent is an important feature of the equatorial ocean. It is typically about 300 km in width and 100 m in depth, with a maximum speed of about 1 m/s. Non-linear advective accelerations are generally thought to be very important in the undercurrent. Nevertheless most of the theories that have been developed are linear, although there are a few examples of non-linear modelling. One such non-linear model is that of Fofonoff (1954). In this model Fofonoff studied the circulation set up in a rectangular basin with a given distribution for the potential vorticity. This led Fofonoff and Montgomery (1955) to note that if friction is small, then using the potential vorticity equation, it should be possible to predict the vorticity of fluid particles in the undercurrent from a knowledge of where the particle originated. Fofonoff and Montgomery considered an example where the undercurrent on each side of the equator originated from a specific latitude on that side of the equator. Using the fact that the undercurrent is zonal and so the zonal gradient of meridional velocity does not contribute to the vorticity, they obtained the zonal velocity field. Unfortunately in their model, because particles either side of the equator have different origins, there is a discontinuity of vorticity at the equator. Ichiye (1964) has pointed out that frictional forces can be expected to smooth this discontinuity. He introduced a new vorticity distribution without such a discontinuity and studied the resultant undercurrent. Despite this the new vorticity distribution which he introduced does not give an undercurrent of the form observed in field observations.

For the purpose of most studies of the equatorial ocean, it is generally assumed valid to neglect the Lagrangian variations in the density of the particles making up the equatorial undercurrent, as they move eastward with the undercurrent flow. Thus from the zonal variations in the density structure of the equatorial oceans (see for example Lemasson and Piton, 1968, cited by Gill, 1975), it appears that in both the Pacific and Atlantic Oceans the equatorial undercurrent flows in a layer which is thicker in the west than the east. The purpose of the present study is to investigate the influence of changes in the thickness of layer through which the undercurrent flows upon the undercurrent. Because the meridional form of the undercurrent is not represented well by the potential vor-

[1] Present address: Australian Numerical Meteorology Research Centre, P.O. Box 5089AA, Melbourne, Victoria, Australia 3001.

0040-2826/79/050447-09$02.50/0 © 1979 Munksgaard, Copenhagen

ticity distributions of Fofonoff and Montgomery or Ichiye, several new potential vorticity distributions are considered here.

2. Formulation

The equatorial ocean is represented here by a simple three-layer model. These layers correspond to the mixed surface layer, the thermocline and the body of the water below the thermocline. All layers are taken to be of constant but different density. The surface and lower layers are assumed to be moving slowly compared with the centre layer. This layer is assumed to contain the equatorial undercurrent. A pressure gradient is maintained in the surface layer by a constant zonal wind stress. The entire system is taken to be frictionless and steady. This study concerns itself with the centre layer.

In any layer of a frictionless steady layered ocean model, the potential vorticitiy, stream function and Bernoulli head are all conserved following a streamline. Hence once a relation between any two of these variables is known at one section through which all streamlines pass, the relation must hold at all subsequent sections. In the studies mentioned in the introduction it was easier to consider a relation between the potential vorticity and stream function when studying the behaviour of the layer containing the undercurrent. However, when the layer thickness varies with the pressure in the layer and the flow is geostrophic in one direction, it is easier to use the potential vorticity and the Bernoulli head. Such is the case of the centre layer to be studied here.

Suppose the relation between the potential vorticity and the Bernoulli head is

$$\frac{-\dfrac{\partial u}{\partial y}+\dfrac{\partial v}{\partial x}+\beta y}{H}=f_B(\tfrac{1}{2}(u^2+v^2)+p) \tag{1}$$

where f_B is a function to be specified, u and v are the zonal and meridional velocities and H is the layer thickness which is a function of the layer kinematic pressure (pressure divided by density), p. β is the meridional gradient of the coriolis parameter and y is the meridional distance from the equator.

Provided vertical accelerations are small the depth of each layer may be determined by hydrostatic balance. For the model as just described, this enables the layer thickness to be written as

$$H=H_\infty+p\cdot\left(\frac{1}{g_{12}}+\frac{1}{g_{23}}\right) \tag{2}$$

where g_{12} and g_{23} are the reduced gravitational accelerations between the upper and centre layers and the centre and lower layers. H_∞ is the layer thickness at the edge of the undercurrent where p is arbitrarily chosen to be zero. H_∞ is a function of x only and its variation with x is determined by the zonal wind stress.

As discussed in the introduction, it has been well established in the literature on the topic that the undercurrent is strongly zonal; that is the zonal velocity and distance scales are much larger than the meridional velocity and distance scales. Also the zonal velocity of the undercurrent is often in geostrophic balance. Hence

$$u=-\frac{1}{\beta y}\frac{\partial p}{\partial y} \tag{3}$$

Philander (1973) discussed the evidence for this assumption.

These assumptions concerning the zonal behaviour of the undercurrent enable eq. (1) to be written as

$$\frac{1}{\beta}\frac{\partial}{\partial y}\left(\frac{1}{y}\frac{\partial p}{\partial y}\right)+\beta y=Hf_B\left(\frac{1}{2\beta^2}\cdot\frac{1}{y^2}\cdot\left(\frac{\partial p}{\partial y}\right)^2+p\right) \tag{4}$$

Apart from the dependence of H on x, this equation is independent of x. Thus for any fixed x, the equation may be integrated to determine the meridional variation of the kinematic pressure, p. Outside the undercurrent p is zero.

The flow between any two streamlines must be conserved and this is embodied in eq. (4). To show this, note that if η is the Benoulli head

$$\frac{\partial\eta}{\partial y}=\frac{1}{\beta y}\frac{\partial p}{\partial y}\cdot\left(\frac{\partial}{\partial y}\left(\frac{1}{\beta y}\frac{\partial p}{\partial y}\right)+\beta y\right) \tag{5}$$

and so eq. (4) becomes

$$\beta y\frac{\partial\eta}{\partial p}=Hf_B(\eta) \tag{6}$$

Equation (6) is a form of an equation first noted in Fofonoff (1954) which relates the potential vor-

ticity, stream function and Bernoulli head. Using eq. (3) it enables the flow between any two energy levels (that is Bernoulli heads), η_1 and η_2, to be written as

$$\int_{\eta_1}^{\eta_2} Hu\,dy = -\int_{\eta_1}^{\eta_2} H\frac{1}{\beta y}\frac{\partial p}{\partial y}\,dy$$

$$= \int_{\eta_1}^{\eta_2} H\frac{1}{\beta y}\,dp = \int_{\eta_1}^{\eta_2} \frac{1}{f_b(\eta)}\,d\eta \qquad (7)$$

Now given η_1 and η_2, the right-hand side of eq. (7) is constant. Thus the flow between energy levels η_1 and η_2, which implies two given streamlines, is constant.

It is necessary for later use to note the conditions governing the development of reverse flow. If

$$-\frac{1}{\beta y}\frac{\partial p}{\partial y} = u = 0 \qquad \text{at } y \neq 0, \qquad (8)$$

then eq. (5) implies

$$\frac{\partial}{\partial y}\left[\frac{1}{2\beta^2 y^2}\cdot\left(\frac{\partial p}{\partial y}\right)^2 + p\right] = \frac{\partial}{\partial y}\eta = 0, \qquad (9)$$

provided the potential vorticity remains finite. The occurrence of eq. (9) does not imply eq. (8) because the zero of eq. (9) may be associated with a zero in potential vorticity. In many examples such a zero occurs only on the equatorial streamline and then the converse argument holds away from the equator.

3. Solution for different energy-vorticity relations

It is useful to non-dimensionalize the problem before proceeding further. Let the distance scale be ζ and the time scale be $1/\beta\zeta$ where ζ is some arbitrary distance. Equation (4) then becomes

$$\frac{\partial}{\partial y}\left(\frac{1}{y}\frac{\partial p}{\partial y}\right) + y = Hf_B\left(\frac{1}{2y^2}\left(\frac{\partial p}{\partial y}\right)^2 + p\right) \qquad (10)$$

Once the form of f_B is specified, the form of the undercurrent can be determined. Two undercurrents (currents 1 and 2) are considered here and another one (current 3) later. The undercurrents considered here are

current 1

$$f_B(\eta) = \frac{1}{H_0}\sqrt{\frac{\eta_0}{\eta} - 1}, \qquad 0 \leqslant \eta \leqslant \eta_0, \qquad (11)$$

and current 2

$$f_B(\eta) = \frac{1}{H_0}\sqrt{\ln\frac{\eta_0}{\eta}}, \qquad 0 \leqslant \eta \leqslant \eta_0 \qquad (12)$$

To simplify the problem, in both these undercurrents η is restricted to decrease monotonically with $|y|$. Hence according to the argument relating eq. (8) to eq. (9), no reverse flow occurs.

H_0 is a standardizing depth and can be chosen arbitrarily. η_0 is a measure of the intensity of the undercurrent and can also be chosen arbitrarily, provided η_0 is positive. (If η_0 is negative, the inequalities on the range of η need to be reversed.) Here only undercurrents for which η_0 is positive are considered.

It can be seen from eq. (11) and eq. (12) that with both undercurrents that have been introduced, when η is at its upper limit, η_0, the potential vorticity, is zero. This corresponds to equatorial conditions. The contour $\eta = 0$ marks the streamline at the outer boundary of the undercurrent. For currents 1 and 2 the potential vorticity is infinite on this streamline. Truncation at an earlier streamline (i.e. placing the boundary of the current where $\eta \neq 0$) where the potential vorticity is not infinite, is considered later. However infinite vorticity, and hence by eq. (3) infinite curvature in the pressure profile, does not cause an infinity in the current speed.

Suppose that the flow on either side of the undercurrent is at rest. The boundary conditions on eq. (10) are then

$$p = 0 \quad \text{at } \eta = 0 \qquad (13)$$

on both sides of the undercurrent. Using symmetry about the equator, the integration of eq. (10) need only be carried out for $y \geqslant 0$.

In eqs. (11) and (12) the restriction was made that η ranges from 0 to η_0 monotonically decreasing as $|y|$ increases. Suppose the integration of these equations is started from $y = 0$, using the starting value $p = p_0$, then the integration can terminate because either

$$\text{(i)}\ \frac{\partial \eta}{\partial y} = 0 \qquad (14)$$

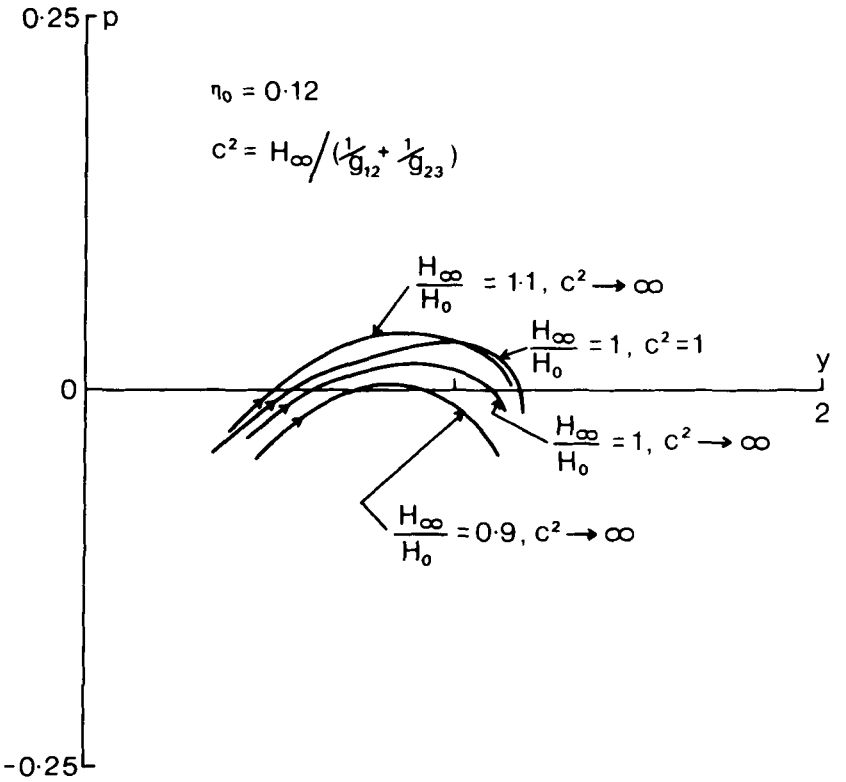

Fig. 1. The relationship between the half width and kinematic pressure at the edge of current 1. This was obtained by integrating eq. (10) and eq. (11) for various values of the pressure at the equator. All values are dimensionless.

reverse flow develops, η fails to decrease monotonically; or

$$\text{(ii)}\quad \eta = 0 \tag{15}$$

the outer streamline is reached.

Figs. 1 and 2 show the loci of the termination point in (y, p) space as p_0 varies, for the various currents. All integrations were carried out numerically by the Runge–Kutta method. Above the line $p = 0$, these loci correspond to termination because eq. (14) is satisfied. This can be seen by noting that $1/2y^2 \cdot (\partial p/\partial y)^2$ and p must both be positive above $p = 0$. Hence $\eta = 1/2y^2 \cdot (\partial p/\partial y)^2 + p$ must be positive and not zero, and so eq. (15) cannot be satisfied. According to eq. (8) and eq. (9), the solution of eq. (10) would show reverse flow if integration was carried on past a point on the loci. Below the line $p = 0$, on the other hand, termination is caused by eq. (15) being satisfied. To see this, suppose $\partial\eta/\partial y = 0$, then $(1/y)(\partial p/\partial y) = 0$ (see the note after eq. (9) for conditions). Thus $\eta = p$. However p is negative for points on the loci below $p = 0$ and so η must be negative. Equation (15) restricts η to being of the one sign, namely positive, and so there is a contradiction. Hence the initial assumption that $\partial\eta/\partial y = 0$ at a point on the loci below $p = 0$ must be wrong. Hence eq. (15), rather than eq. (14), must be satisfied on the loci below $p = 0$. A solution exists when $p = 0$ on the locus, as both eq. (14) and eq. (15) are satisfied simultaneously. Hence boundary conditions, eq. (13), are satisfied.

In the case of currents 1 and 2 which behave very similarly to each other, it can be seen that two currents can exist. Starting within the single-solution regime, as the depth decreases (that is H_∞/H_0 decreases), the single-solution regime becomes a two-solution regime and then finally a no-solution regime, as seen from the number of intersections of the locus with $p = 0$. When two solutions are present, it is easy to see that one current narrows and one current widens as the depth of the layer changes. From eq. (7), it follows that both solu-

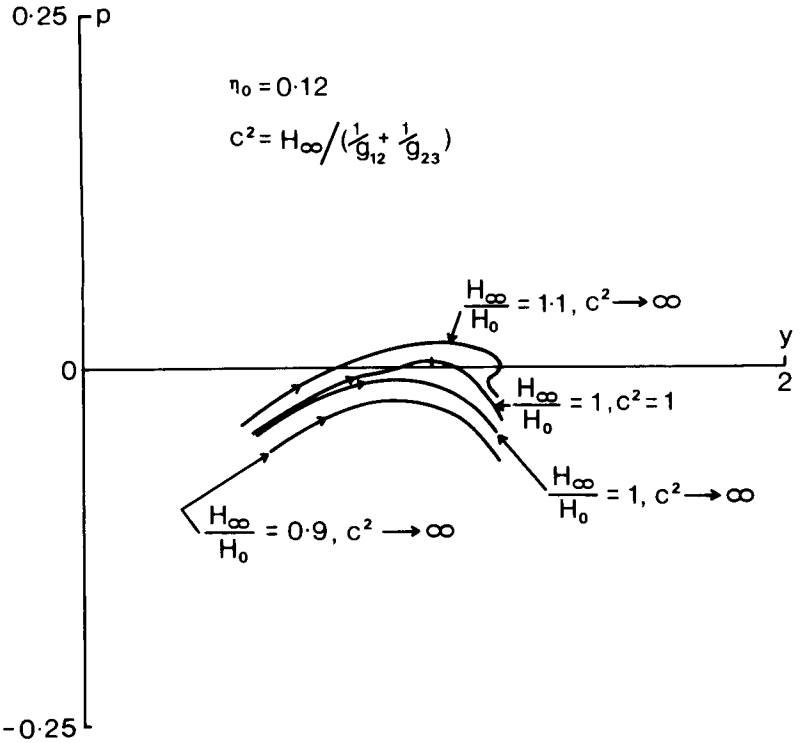

Fig. 2. The relationship between the half width and kinematic pressure at the edge of current 2. This was obtained by integrating eq. (10) and eq. (12) for various values of the pressure at the equator. All values are dimensionless.

tions convey the same mass flux of water within a given energy range.

The behaviour of the undercurrent when there are two possible solutions has an analogy in open channel flow (Streeter, 1971). In open channel flow there are two possible solutions for a given mass transport. One of these solutions represents a deep slow flow while the other solution represents a shallow fast flow. If the width of the channel in which this flow occurs is increased, the deeper flow shallows while the shallow flow deepens. The analogous description for the equatorial undercurrent when there are two solutions is that one of the solutions represents a wide slow flow while the other solution represents a narrow fast flow. If the depth of the layer in which this flow occurs is decreased, the wider flow narrows while the narrow flow widens.

When the integration stops above $p = 0$, say at $p = p_T > 0$, it does so with $\partial p/\partial y = 0$, as discussed in the paragraph after eq. (15). Such a zero gradient in the pressure corresponds to a zero zonal velocity because $u = -(1/y)(\partial p/\partial y)$. This point can be made to correspond to the outer streamline conditions of a current by considering the far field to be at a pressure p_T rather than 0. This merely involves changing the datum of the pressure. The range of integration is then not from $0 \leqslant \eta \leqslant \eta_0$, but from $p_T \leqslant \eta \leqslant \eta_0$. This change of the energy of the termination point from $\eta = 0$ to $\eta = p_T$ means that the current now terminates with a finite vorticity. It can be seen from Figs. 1 and 2 that a single-current regime with termination occurring when $\eta = 0$ often becomes a two-current regime when termination occurs at $\eta = p_T$. With very high values of p_T, a no-current regime is encountered according to Figs. 1 and 2. Thus the double current structure is not directly related to having a large potential vorticity streamline at the outer boundary as in currents 1 and 2. The double current structure is tied closely with the particular distribution of potential vorticity with stream function or energy.

In Figs. 1 and 2, C^2 has been specified as $H_\infty/(1/g_{12} + 1/g_{23})$. C^2 is thus a measure of the

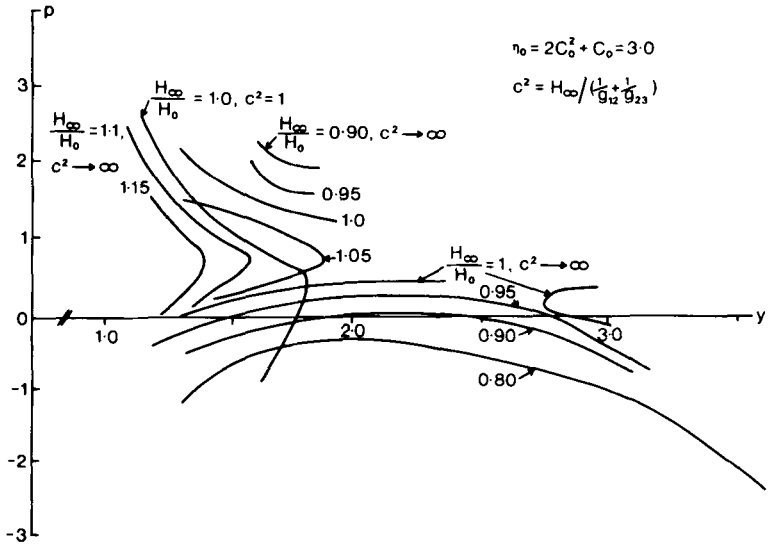

Fig. 3. The relationship between the half width and kinematic pressure at the edge of current 3. This was obtained by integrating eq. (10) and eq. (16) for various values of the pressure at the equator. All values are dimensionless.

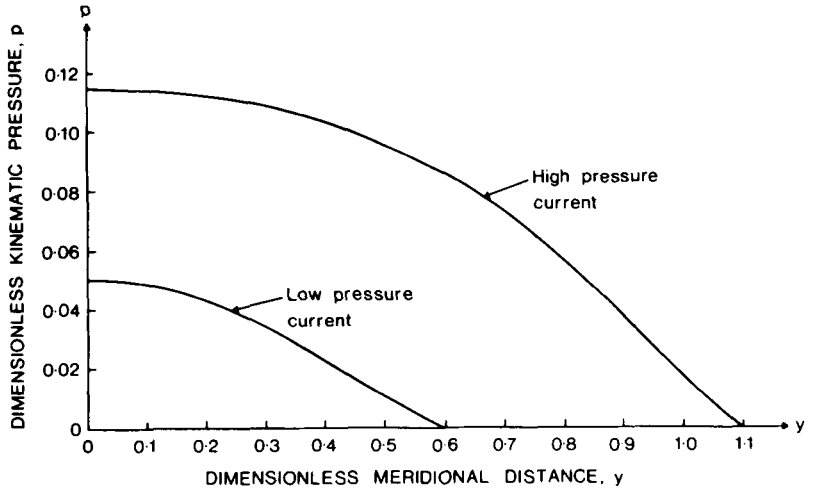

Fig. 4. The relationship between the kinematic pressure and meridional distance from the equator for the low and high pressure currents of form current 1 when $H = H_0$. Note the smooth behaviour of the solutions. Both of these currents have the same zonal mass flux associated with them.

baroclinic response of the system. When C^2 is large the model behaves barotropically. When C^2 is small the model behaves baroclinically. It can be seen from Figs. 1 and 2 that baroclinic behaviour moves the loci upwards, thus effectively increasing the value of H_∞/H_0, hence H. This result can be inferred for an eastward flowing undercurrent (p is positive in such a current) from eq. (2) and the definition of C^2. If the current were westward flowing, p would be negative and H would be decreased.

It is constructive to consider one other function, f_B, giving a third current. The function for current 3 is

$$f_B(\eta) = \frac{1}{H_0} \cdot \left(\frac{8C_0}{\phi^3} + 1 \right) \cdot \sqrt{\phi - 1}, \qquad (16a)$$

where ϕ is given by the root greater than or equal to 1 of

$$\phi^4 \eta - \phi^3 C_0 - 2C_0^2 = 0 \qquad 0 \leqslant \eta \leqslant \eta_0 = C_0^2 + C_0 \tag{16b}$$

with η again decreasing monotonically with $|y|$ so as to avoid reverse flow by eq. (9). This relationship defining f_B may seem needlessly complicated, but it has in its favour that it admits the solution

$$p = \frac{C_0}{y^2 + 1}, \tag{17}$$

when $H = H_0$ for all y. By eq. (7), this current is transporting the same flow as any other currents which result from eq. (16). By eq. (3) this flow is $-h_0 \int_0^\infty (1/y)(\partial p/\partial y)\, dy$ on each side of the equator. Substituting eq. (17) to eliminate p gives the flow in terms of C_0 and H_0. The resulting integral, when evaluated by contour integration around the upper half of the complex y-plane, gives this flow as $(\pi/2) C_0 H_0$ on each side of the equator. It can be seen from eq. (17) that for the current given by eq. (16), the distance scale, ζ, is the distance at which the pressure falls to one half of its equatorial value.

As before in Figs. 1 and 2, the locus of the termination point is plotted in (y, p) space, Fig. 3. The behaviour is similar to that of currents 1 and 2. However when $H = H_0$, the locus distorts to include the solution of eq. (17). In the region of high p, the curve truncates at low y because an inflection point develops in the p profile and this ultimately gives reverse flow, as discussed below.

Two further points are worth noting. Firstly, in order to obtain a similar behaviour, discussed above, from the various currents, the values of C_0 (defined by $\eta_0 = 2C_0^2 + C_0$) are much higher for this current, current 3, than for currents 1 and 2. All these three currents have the same range of vorticity.

For $C_0 > 0.4696$, there is a range of vorticity for which the function, f_B^{-1}, associated with current 3 is not single-valued. Thus rather than increase monotonically with $|y|$, the vorticity decreases over part of the range of $|y|$. The effect of this on the undercurrent pressure profile can be seen in Fig. 4 and Fig. 5 as a strong inflection where there is only a low velocity in the high pressure solution of current 3 which is lacking in current 1. This may explain the high value of C_0 required by this current to obtain a similar behaviour to currents 1 and 2.

Secondly, the solution corresponding to eq. (17) fails to exist for $H \neq H_0$. This is explained by considering the flow in which a small finite variation, δH, in H occurs within a finite change in x. This suggests a variation in y following a particle of $\delta y = y(\delta H/H)$ at large $|y|$, so that the potential vorticity, which is approximately $\beta y/H$ at large $|y|$, remains constant on streamlines. Hence $v \sim uy(\partial H/\partial x)(1/H)$, which for large $|y|$ contradicts

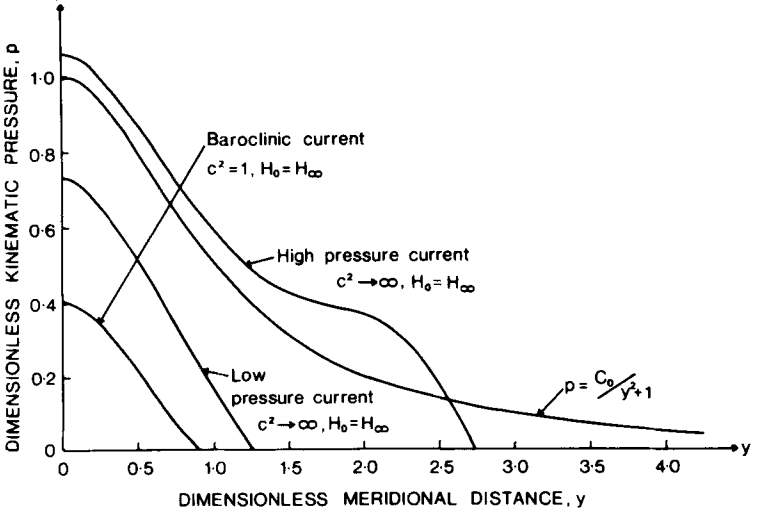

Fig. 5. The relationship between the kinematic pressure and meridional distance from the equator for the various forms of current 3 where $H_0 = H_\infty$ and $C_0 \to \infty$ or $C_0 = 1$. Note the distortion of the high pressure current. All of these currents transport the same zonal mass flux.

the assumption of strong zonal behaviour. Hence the derivation of eq. (4) breaks down. This does not mean that a current of the form eq. (17) cannot exist. It merely means that the theory presented here is invalid in studying such a current.

4. Discussion

Fofonoff (1954), Fofonoff and Montgomery (1955) and Ichiye (1964) have all carried out investigations of the flow pattern generated by a given distribution of potential vorticity with stream function. By choosing a linear distribution of potential vorticity, they solved linear equations to obtain a unique flow pattern. Here it has been shown that for a given distribution of potential vorticity with stream function or Bernoulli head, the flow pattern is not necessarily unique.

Depending on the distribution of potential vorticity, the layer thickness and the extent of baroclinicity, two solutions for the equatorial undercurrent may be possible. As the layer thickness decreases, the narrower of the two solutions widens, while the wider of the two solutions narrows. Eventually some critical depth is reached at which the two solutions coalesce to give a single solution. This solution then vanishes with further decreases of the layer thickness. This behaviour is in some ways analogous to open channel flow, as discussed earlier. An increased baroclinic behaviour effectively increases the layer thickness.

The width of the observed equatorial undercurrent does not vary greatly along the equator, but remains constant at about 300 km $\pm$ 100 km. However, the model given here suggests the width is sensitive to the thickness of the layer containing the undercurrent. This implies that either there is little zonal change in the layer thickness (assuming the continuously stratified ocean can be validly approximated by a layered ocean) or the equatorial undercurrent is dominated by friction. Based on observations of the persistence of the high velocities in the undercurrent, especially in the Atlantic and Pacific Oceans, it seems unlikely that the latter is true although it cannot be totally dismissed as a reason for the breakdown of the model.

The thickness of the layer through which the undercurrent flows does, however, decrease towards the east was noted in the introduction. This provides a dilemma. A possible explanation of the dilemma may be that the density of a particle in the undercurrent does not remain constant and so the changes in the density structure of the equatorial ocean do not indicate whether vortex lines are being compressed or stretched. In addition such density changes may enable a meridional circulation to be established—as is found in most homogeneous models of the undercurrent (Gill, 1975). Such a meridional circulation may also influence the structure of the undercurrent.

The non-linear behaviour of the equatorial undercurrent is extremely complex. This study highlights the complicated behaviour which can be obtained from non-linear models of the equatorial undercurrent.

5. Acknowledgments

I wish to express my gratitude to Dr. A. E. Gill, for his constant helpful advice while supervising this study. This study was financed by the Royal Commission for the Exhibition of 1851 and I wish to thank the Commissioners for their support.

REFERENCES

Fofonoff, N. P. 1954. Steady flow in a frictionless homogeneous ocean. *J. Mar. Res. 13*, 254–262.

Fofonoff, N. P. and Montgomery, R. B. 1955. The equatorial undercurrent in the light of the vorticity equation. *Tellus 7*, 518–521.

Gill, A. E. 1975. Models of the equatorial currents. In *Numerical models of ocean circulation.* National Academy of Science, 181–203.

Ichiye, T. 1964. An essay of the equatorial current system. In *Studies on oceanography* (ed. K. Yoshida), pp. 38–46. Seattle: University of Washington Press.

Lemasson, L. and Piton, B. 1968. *Cah. ORSTOM, Ser. Oceanogr. 6*, 39–46.

Philander, S. G. H. 1973. Equatorial undercurrent: measurements and theories. *Rev. Geophy. and Space Phy., 11*, 513–570.

Streeter, V. L. 1971. *Fluid mechanics*, 5th ed. New York: McGraw-Hill.

УТОНЬШЕНИЕ ЭКВАТОРЙАЛЬНОГО ГЛУБИННОГО ПРОТИВОТЕЧЕНИЯ

Путем использования трех различных распределений потенциального вихря показано, что поле скорости в экваториальном глубинном противотечении определяется неоднозначно. Единственность поля скоростиявляется функцией как толщины слоя, через который проходит течение, так и распределения потенциального вихря. Для распределений, изучаемых здесь, имеется одно решение для большой толщины слоя. По мере убывания толщины слоя формируется второе решение. Эти два решения затем сливаются и исчезают по мере дальнейшего уменьшения толщины слоя. Рост бароклинности качественно приводит к тому же эффекту, что и рост толщины слоя. Когда присутствуют два решения, более узкое решение расширяется по мере убывания толщины слоя, тогда как более широкое решение сужается.